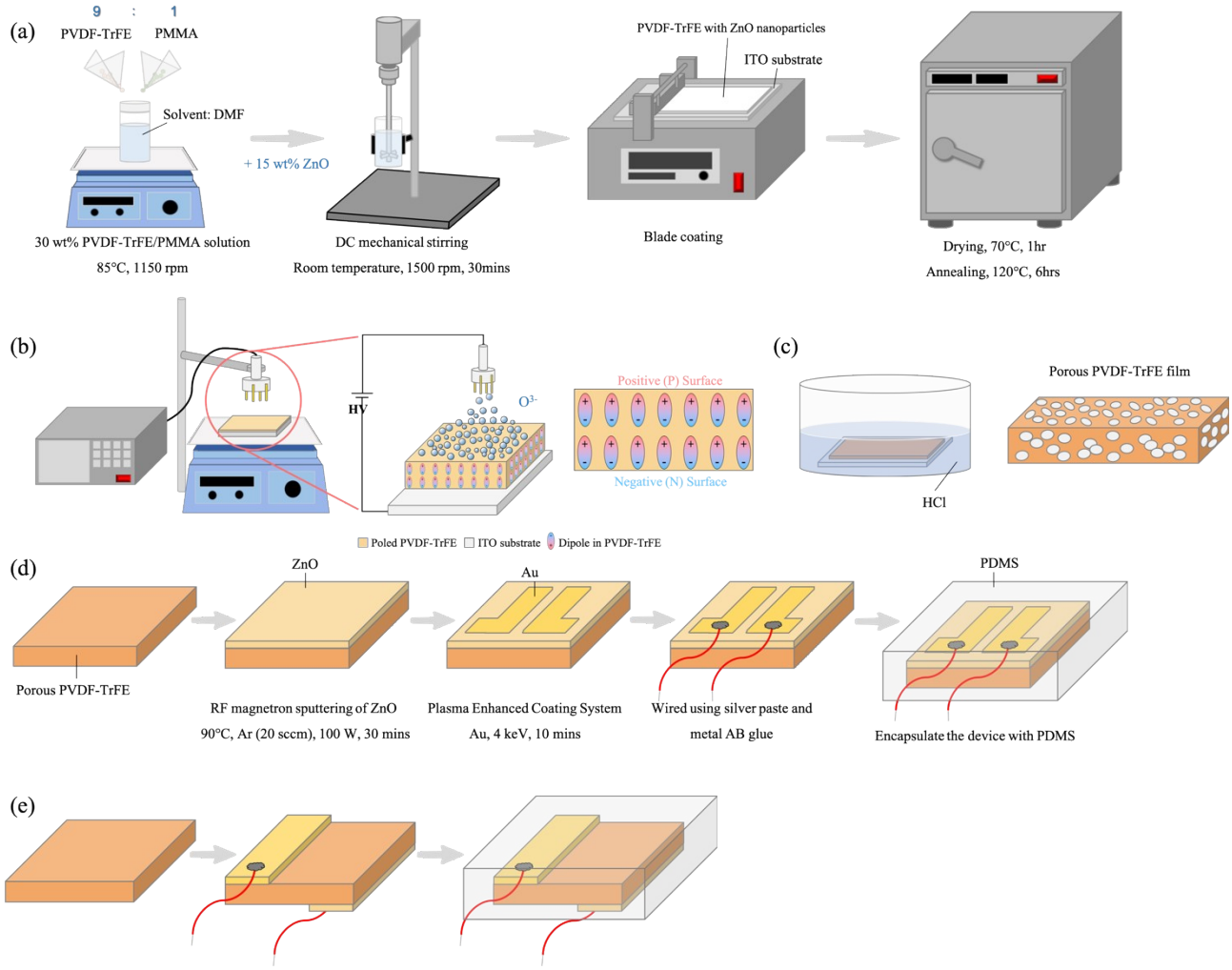

Figure S1. Schematic diagram of (a) the fabrication process of the PVDF-TrFE/ZnO nanoparticle composite thin film, (b) the corona poling process and the resulting surface charges in PVDF-TrFE with ZnO nanoparticles, (c) the selective etching of ZnO nanoparticles using HCl, and the fabrication of the (d) PGTFT and (e) porous PVDF-TrFE film based PENGdevice.

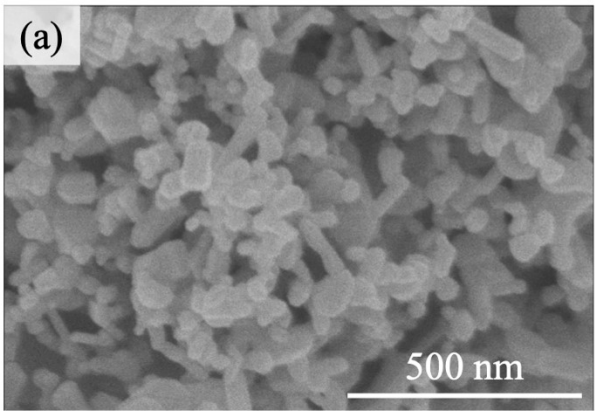

(b)

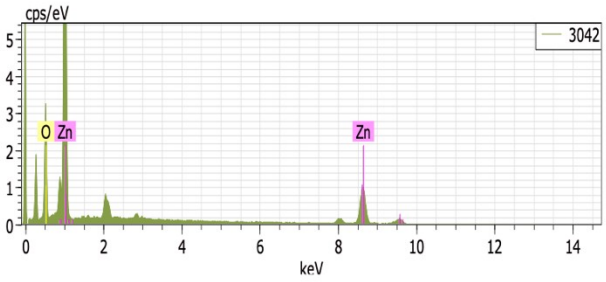

Element	Atomic concentration (at.%)
Zn	51.14
O	48.86
Total	100

Figure S2. (a) SEM image of commercial ZnO nanoparticles and (b) the corresponding EDS spectrum and elemental table.

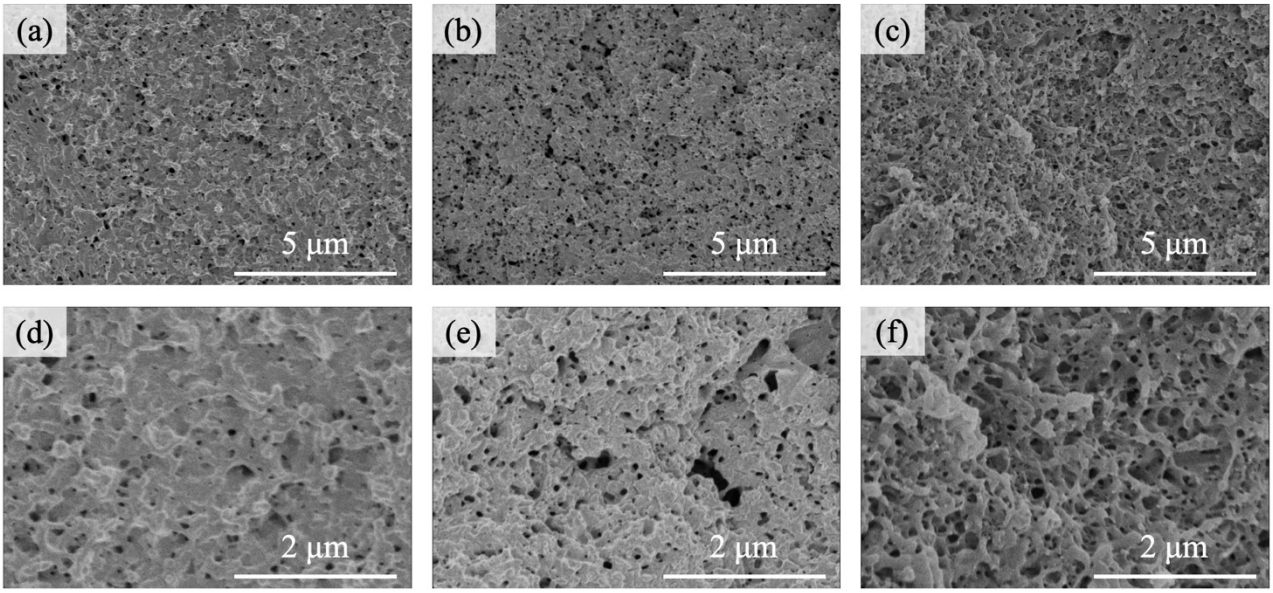

Figure S3. Cross-sectional SEM images at different magnifications for PVDF-TrFE films containing (a, d) 5 wt% ZnO, (b, e) 15 wt% ZnO, and (c, f) 25 wt% ZnO.

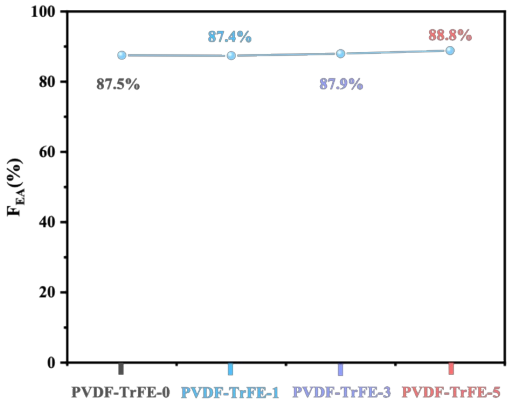

Figure S4. Electroactive β-phase fraction of PVDF-TrFE films with different poling duration.

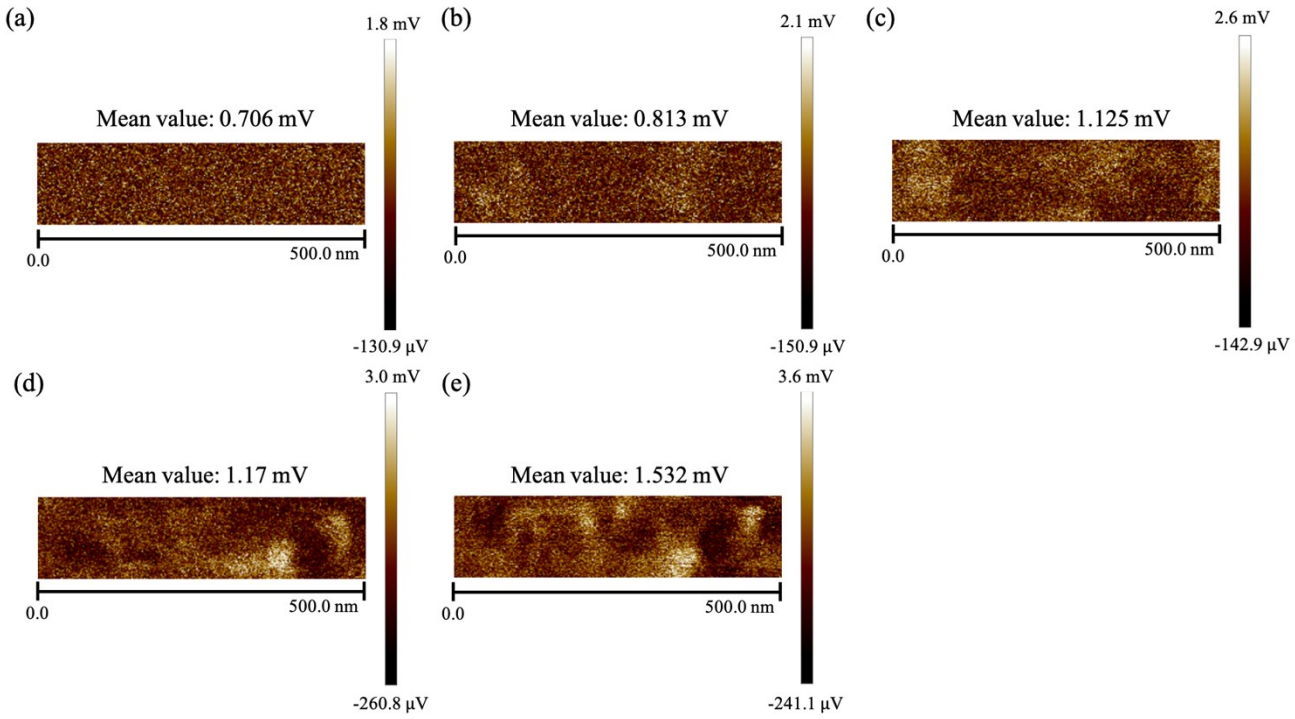

Figure S5. Piezoelectric amplitude mappings obtained by PFM for unpoled PVDF-TrFE under applied biases of (a) 1 V, (b) 3 V, (c) 5 V, (d) 7 V, and (e) 9 V.

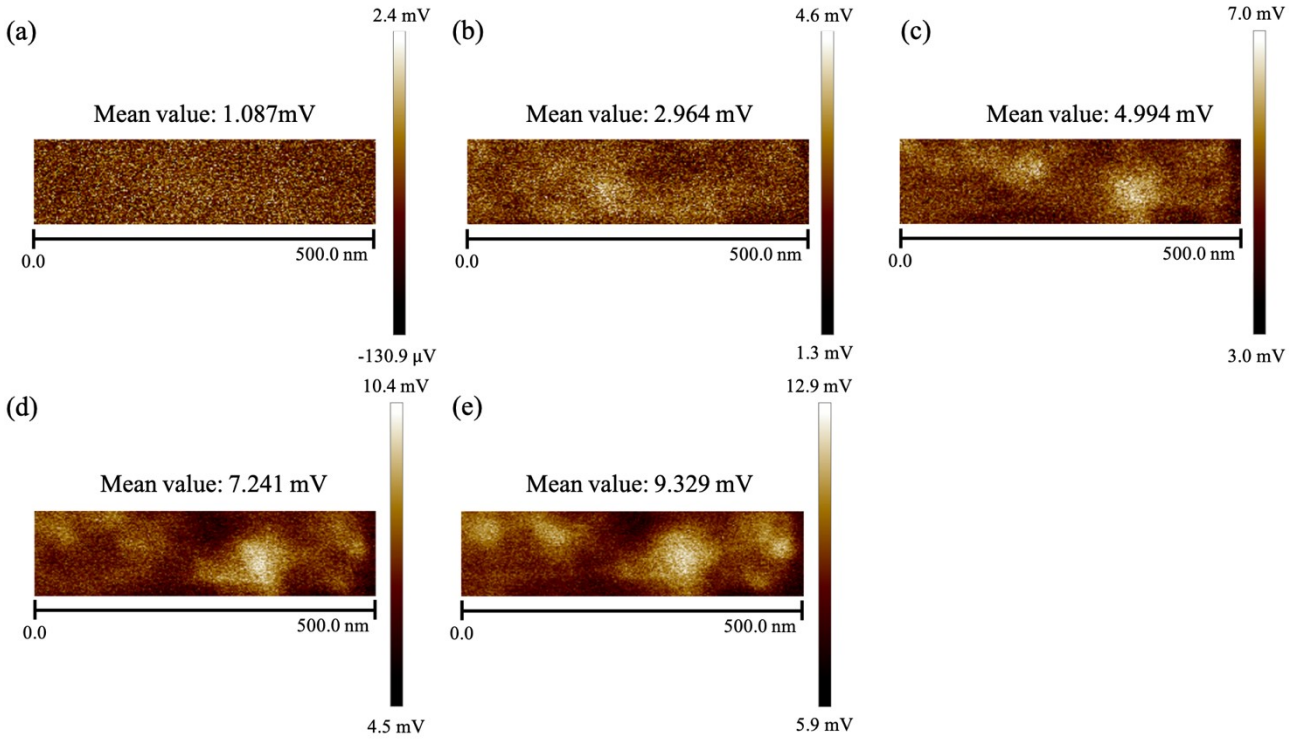

Figure S6. Piezoelectric amplitude mappings obtained by PFM for PVDF-TrFE-1 under applied biases of (a) 1 V, (b) 3 V, (c) 5 V, (d) 7 V, and (e) 9 V.

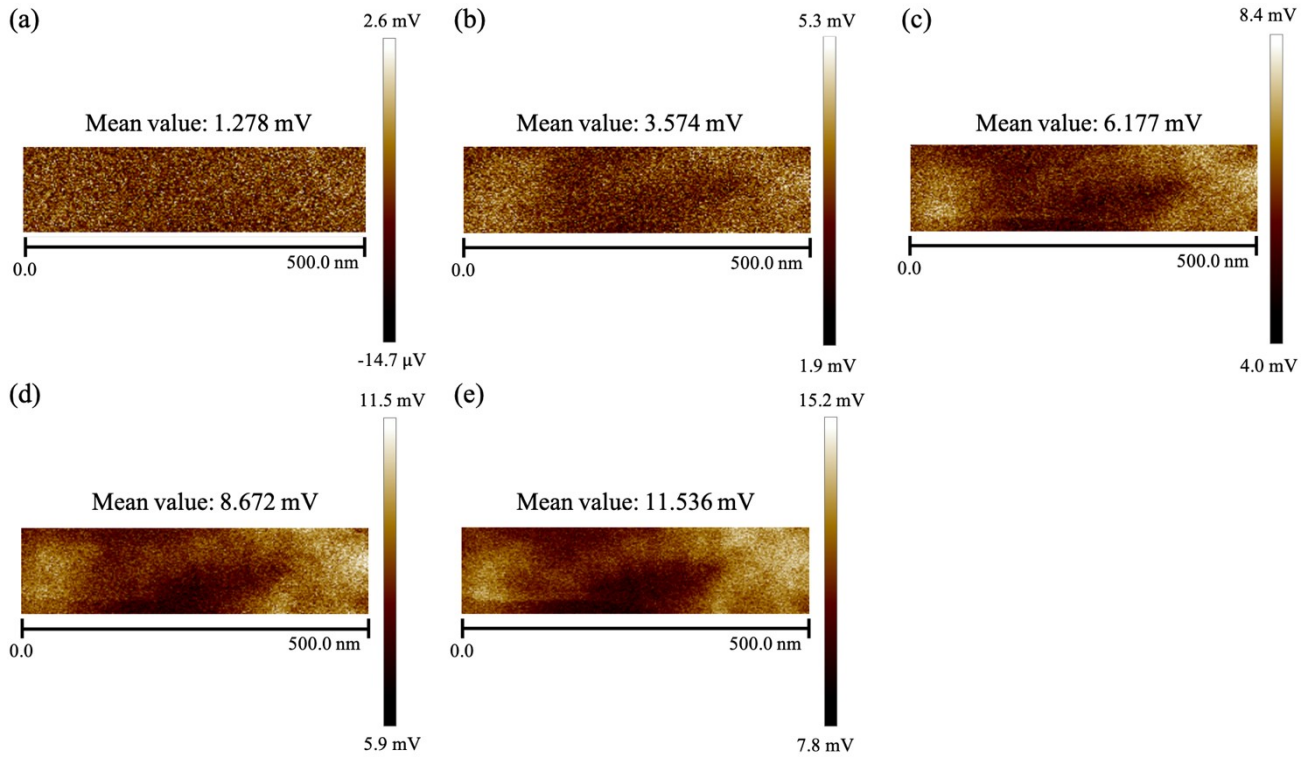

Figure S7. Piezoelectric amplitude mappings obtained by PFM for PVDF-TrFE-3 under applied biases of (a) 1 V, (b) 3 V, (c) 5 V, (d) 7 V, and (e) 9 V.

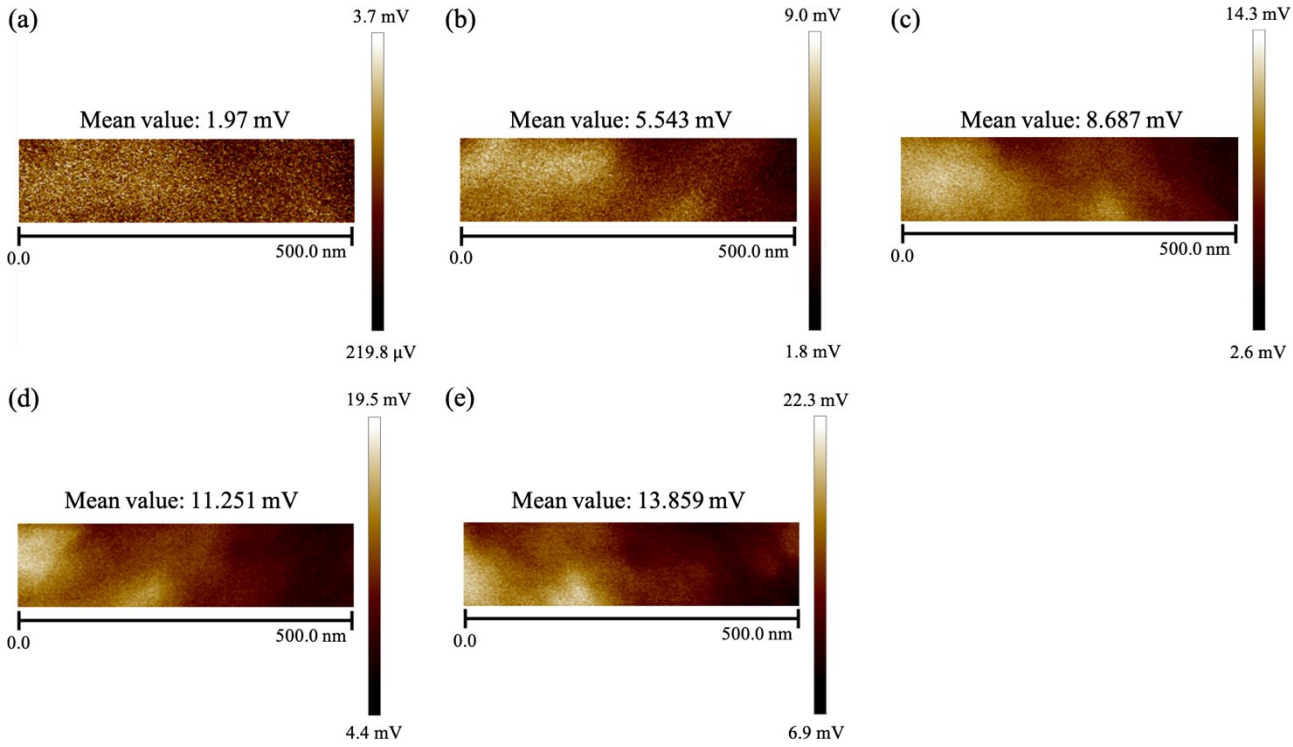

Figure S8. Piezoelectric amplitude mappings obtained by PFM for PVDF-TrFE-5 under applied biases of (a) 1 V, (b) 3 V, (c) 5 V, (d) 7 V, and (e) 9 V.

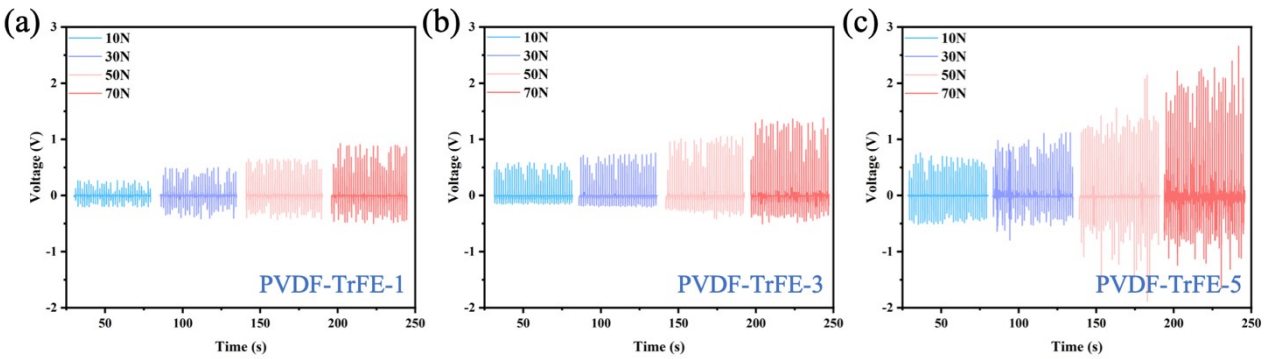

Figure S9 (a) Open-circuit voltage of (a) PVDF-TrFE-1, (b) PVDF-TrFE-3, and (c) PVDF-TrFE-5 PENGs.

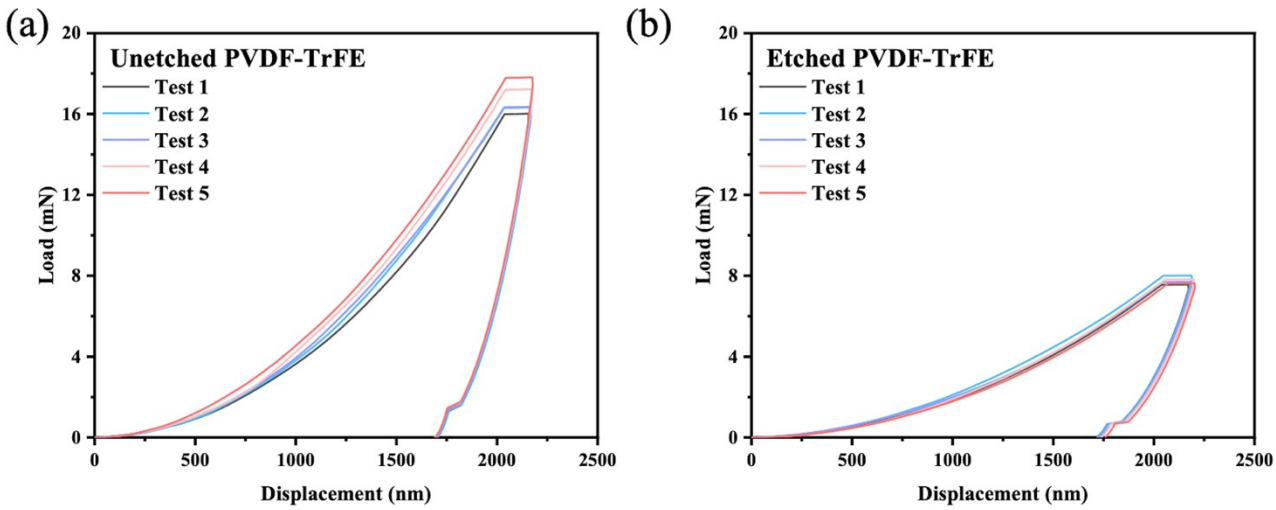

Figure S10. Load-displacement curves of (a) unetched PVDF-TrFE and (b) etched PVDF-TrFE.

	Unetch PVDF-TrFE	**Etched PVDF-TrFE**
Young's Modulus (E)	5.5 GPa	2.5 GPa
Hardness (H)	0.16 GPa	0.08 GPa
Elastic Deformation ($S_{elastic}$)	456.2 nm	468.0 nm

Table S1. Young's Modulus (E), Hardness (H), and Elastic deformation($S_{elastic}$) of unetched and etched PVDF-TrFE.

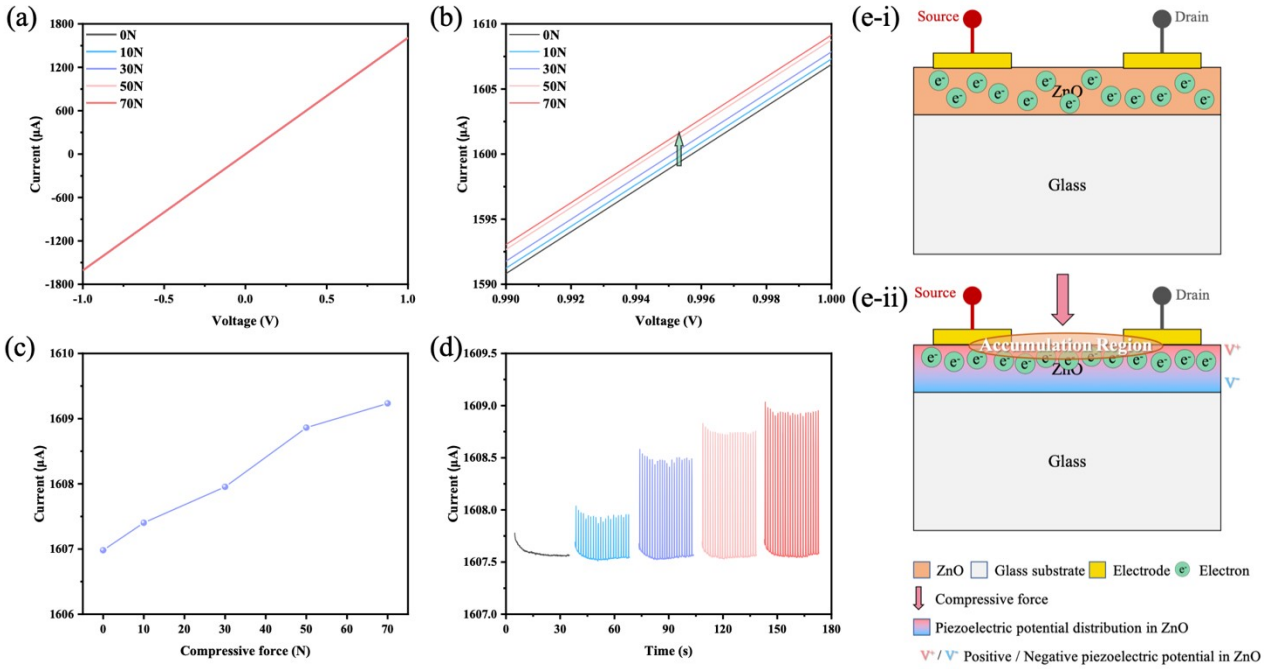

Figure S11. (a) Current-voltage characteristics of ZnO@Glass under different compressive forces. (b) Enlarged view of the I–V curves from (a) in the voltage range of 0.99–1 V. (c) Output current response of ZnO@Glass under varying compressive forces (0–70 N) at a bias of 1 V. (d) Cyclic force-dependent output current of ZnO@Glass at 1V. (e) Schematic illustration of the working mechanism of ZnO@Glass: (e-i) before and (e-ii) after applying compressive force.

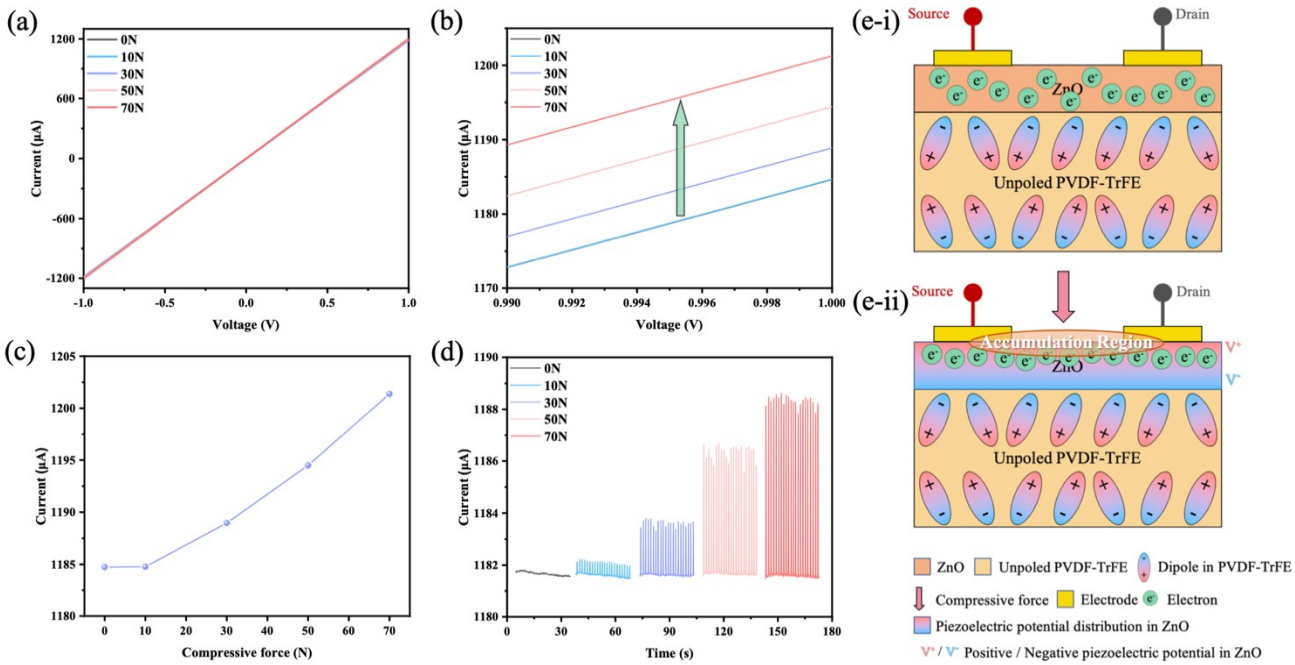

Figure S12. (a) Current-voltage characteristics of ZnO@PVDF-TrFE-0 under different compressive forces. (b) Enlarged view of the I-V curves from (a) in the voltage range of 0.99-1 V. (c) Output current response of ZnO@PVDF-TrFE-0 under varying compressive forces (0–70 N) at a bias of 1 V. (d) Cyclic force-dependent output current of ZnO@PVDF-TrFE-0 at 1V. (e) Schematic illustration of the working mechanism of ZnO@PVDF-TrFE-0 PGTFT: (e-i) before and (e-ii) after applying compressive force.

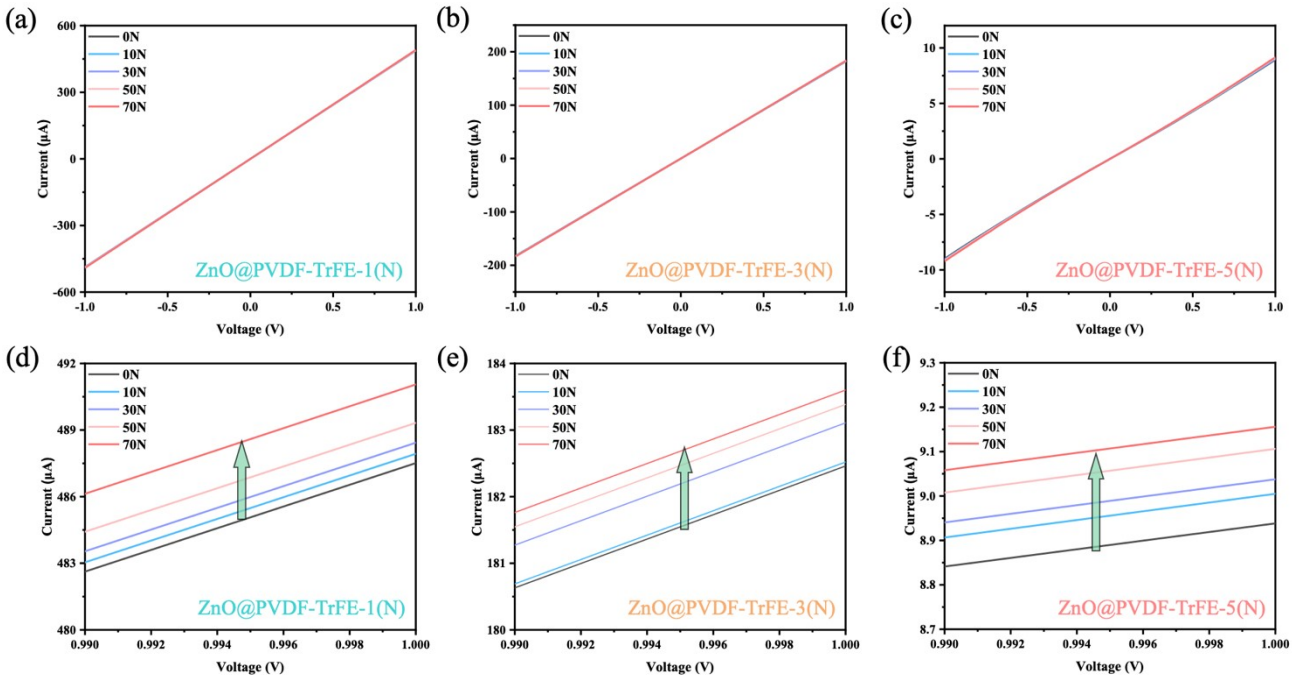

Figure S13. Force-dependent current-voltage characteristics of (a) ZnO@PVDF-TrFE-1(N), (b) ZnO@PVDF-TrFE-3(N), and (c) ZnO@PVDF-TrFE-5(N). Enlarged views of the I–V curves in the voltage range of 0.99–1 V for (d) ZnO@PVDF-TrFE-1(N), (e) ZnO@PVDF-TrFE-3(N), and (f) ZnO@PVDF-TrFE-5(N).

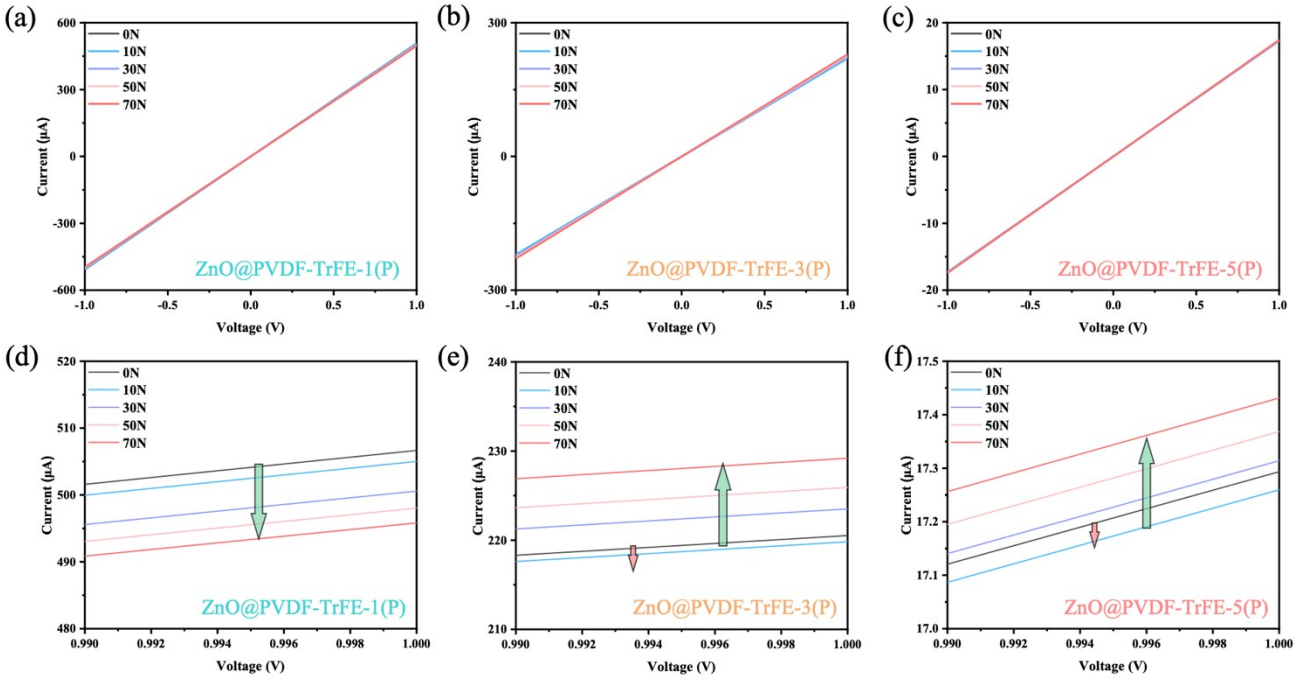

Figure S14. Force-dependent current-voltage characteristics of (a) ZnO@PVDF-TrFE-1(P), (b) ZnO@PVDF-TrFE-3(P), and (c) ZnO@PVDF-TrFE-5(P). Enlarged views of the I–V curves in the voltage range of 0.99–1 V for (d) ZnO@PVDF-TrFE-1(P), (e) ZnO@PVDF-TrFE-3(P), and (f) ZnO@PVDF-TrFE-5(P).

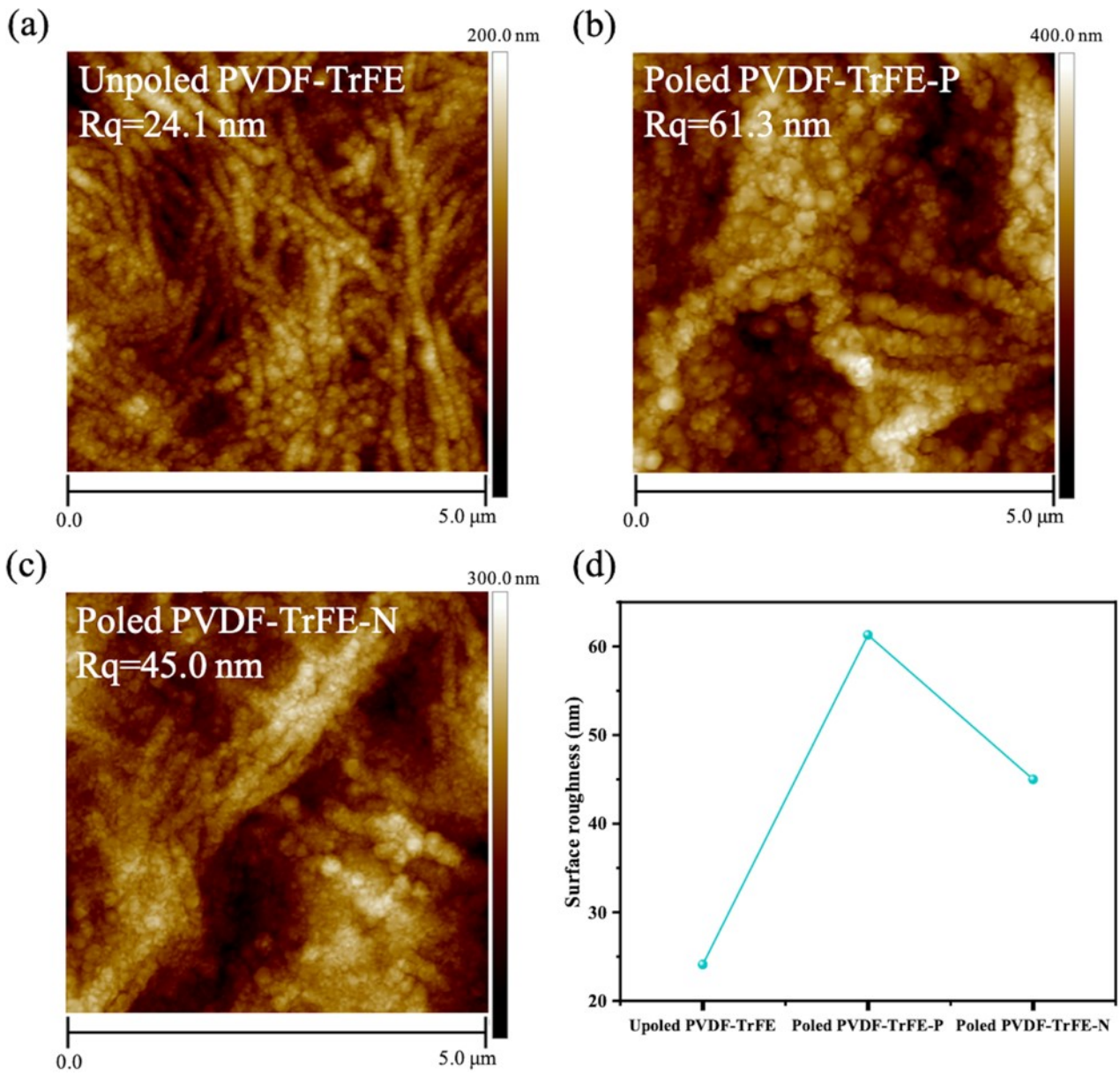

Figure S15. AFM morphology of (a) unpoled PVDF-TrFE, (b) poled PVDF-TrFE-P, (c) poled PVDF-TrFE-N, and (d) the comparison of surface roughness of unpoled PVDF-TrFE, poled PVDF-TrFE-P, and PVDF-TrFE-N.